UC Davis
UC Davis Previously Published Works

Title

Production and Characterization of Biotinylated Anti-fenitrothion Nanobodies and Development of Sensitive Fluoroimmunoassay

Authors

Chen, Zi-Jian
Zhang, Yi-Feng
Chen, Jia-Lin
et al.

Peer reviewed

Production and Characterization of Biotinylated Anti-Fenitrothion Nanobodies and Development of Sensitive Fluoroimmunoassay

Zi-Jian Chen[†,1], **Yi-Feng Zhang**[†,1], **Jia-Lin Chen**[†], **Ze-Shan Lin**[‡], **Min-Fu Wu**[§], **Yu-Dong Shen**[†], **Lin Luo**[†], **Hong Wang**[†], **Xiao-Wei Wen**[†], **Bruce Hammock**[Ψ], **Hong-Tao Lei**[†], **Zhen-Lin Xu**[†,*]

[†]Guangdong Provincial Key Laboratory of Food Quality and Safety/ Research Center for Green Development of Agriculture, South China Agricultural University, Guangzhou 510642, China.

[‡]Guangzhou Institute of Food Inspection, Guangzhou 510410, China

[§]Department of Food Science, Foshan Polytechnic, Foshan 528137, China.

[Ψ]Department of Entomology and UCD Comprehensive Cancer Center, University of California, Davis, California 95616, United States.

Abstract

A simple and sensitive fluoroimmunoassay (FIA) based on a heavy chain antibody (VHH) for rapid detection of fenitrothion was developed. A VHH library was constructed from an immunized alpaca and one clone recognizing fenitrothion (namely VHHjd8) was achieved after careful biopanning. It was biotinylated by fusing with Avi-tag and biotin ligase to obtain a fusion protein (VHHjd8-BT) showing both binding capacity to fenitrothion and streptavidin poly-horseradish peroxidase conjugate (SA-polyHRP). Based on a competitive assay format, the absorbance spectrum of oxidized 3,3',5,5'-tetramethylbenzidine (oxTMB) generated by SA-polyHRP overlapped the emission spectrum of carbon dots, which resulted in quenching of signal by inner filter effect. The developed FIA showed IC_{50} value of 1.4 ng/mL and limit of detection (LOD) of 0.03 ng/mL, which exhibited 15-fold improvement compared with conventional enzyme-linked immunosorbent assay. The recovery test of FIA was validated by a standard GC-MS/MS and the results showed good consistency, indicating the assay is an ideal tool for rapid screening of fenitrothion in bulk food samples.

Keywords

Fenitrothion; Nanobody; Biotinylation; Fluoroimmunoassay; Carbon dots

INTRODUCTION

With the growing population and increasing need for agricultural products, widespread usage of pesticides are necessary and inevitable in modern agriculture to ensure crop yield. [1, 2] However, improper and excessive usage of pesticides may cause their residues in agricultural products as well as soil and water, which may result in pesticide exposure and health risk to human beings. [3, 4] Fenitrothion is a kind of broad-spectrum organophosphate insecticide widely used for preventing agricultural products from insect pests. [4, 5] Many countries and organization have set up strict maximum residue limits (MRLs) for fenitrothion in vegetable and fruit, including China (0.5 mg/kg), [6] EU (0.01 mg/kg), [7] USA (3.0 mg/kg), [8] and FAO (0.5 mg/kg). [9] Conventionally, instrumental methods including high-performance liquid chromatography-tandem mass spectroscopy (HPLC-MS/MS) and gas chromatography-tandem mass spectroscopy (GC-MS/MS) have been well employed for the determination of fenitrothion. [10] Although these methods are precise and sensitive, they always require expensive equipment, well-trained operators, and are time-consuming. They cannot completely fulfill the increasing needs of rapid screening of bulk samples.

Immunoassay is an ideal alternative method for the screening of pesticides owing to the advantages of high sensitivity, specificity, and economy. [11] It has been well developed and approved as standard screening method. [12] Conventional monoclonal antibodies (mAbs) are the main role in the development of immunoassays. Nevertheless, some shortcomings such as complicated cell screening, long productive period, single-function, and high cost have limited their application. In contrast, engineering antibodies expressed from microorganism cells, thereby can be produced on a large scale with a low cost in short period. [13, 14] Heavy chain antibody (VHH) or nanobody is the recombinant variable domain derived from camelidae, [15, 16] which is the smallest class of antibody fragment containing complete antibody function. Unlike other engineering antibodies, such as singe-chain variable fragment (scFv) and fragment antigen binding (Fab), VHHs exhibit high affinity and solubility owing to the avoidance of the complex interaction of heavy chain and light chain in prokaryotic expression systems and the structure is closer to its natural configuration. [15, 17, 18] Moreover, attributed to the special construction, some VHHs were reported to have good stability under extreme conditions like high concentration of organic solvent and high temperature. [19, 20] These unique characteristics made VHH attractive and have a high potential to be an alternative reagent for the next generation of immunoassays.

For the development of VHH-based immunoassay, conventional indirect competitive ELISA (icELISA) is the main analysis method, which however still suffer from the sensitivity limitation. Fluoroimmunoassay (FIA) is a promising and alternative tool showing advantages of high sensitivity, low matrix interference, and wide detection range. [21]

For FIA, fluorescent probe is the key role which mainly decide the method sensitivity. Carbon dots (CDs) are the type of novel nanosized optical materials, [22] and have attracted increasing attention owing to the features of low toxicity, water-solubility, broad sources, and easy synthesis, [23–25] which are the ideal fluorescent materials to develop FIA.

In this work, an alpaca was immunized with the fenitrothion immunogen and the VHH library was constructed for biopanning. The VHH showed the best performance was fused with biotin ligase and Avi-tag to obtain a biotinylation VHH. Streptavidin poly-horseradish peroxidase conjugate (SA-polyHRP) was employed for signal amplification. To further improve the assay sensitivity, red-emission CDs (rCDs) were synthesized and employed to develop FIA. Based on a competitive assay format by using SA-polyHRP, rCDs were subsequently added after generation of oxidized 3,3',5,5'-tetramethylbenzidine (oxTMB) by SA-polyHRP. The fluorescent signal of rCDs can be quantitatively quenched by oxTMB through inner-filter effect, thereby forming a sensitive signal response to fenitrothion. This sensitivity improvement strategy can be easily achieved without extra complex steps, which is simple, time-saving, and effective for fenitrothion analysis. Moreover, the developed FIA will be carefully optimized and further applied for the real sample test to verify the practicality and accuracy.

MATERIALS AND METHODS

Materials and Reagents.

Pesticide standards were purchased from Tanmo Technology Ltd. (Beijing, China). Lactoferrin (LF), bovine serum albumin (BSA), Freund's complete adjuvants, Freund's incomplete adjuvants, and isopropyl-β-d-thiogalactoside (IPTG) were purchased from Sigma (St. Louis, USA). Total RNA extraction kit was purchased from Gbcbio Technologies (Guangzhou, China). First-strand cDNA synthesis kit was obtained from Thermo Fisher Scientific (Shanghai, China). Gel extraction and PCR purification kits were supplied from TIANGEN (Beijing, China). Helper phage M13KO7, *SfiI* restriction enzymes, and T4 DNA ligase were purchased from New England Biolabs (Beijing, China). Primary secondary amine (PSA) was supplied from Biocomma Limited (Shenzhen, China). The pINQ and pCY216 vectors were both generous gifts from Universidad de la Republica de Uruguay. Rabbit anti-camelid VHH antibody-HRP (anti-VHH-HRP) was purchased from GenScript (Nanjing, China). Streptavidin poly-HRP80 conjugate (SA-polyHRP) was supplied from Fitzgerald (Acton, USA). Immunogen (hapten 1-LF), coating antigen (hapten 2-BSA), and anti-fenitrothion monoclonal antibody (mAb) were prepared and stored in our lab. [26] The structure of haptens and artificial antigens are shown in Figure 1A.

Instruments.

PCR was performed in DNA Engine PCR amplifier and DNA was determined by Mini-Sub cell GT system and a Gel imaging system that were all obtained from Bio-Rad (Hercules, CA, USA). Electroporation was performed in Gene Pulser Xcell electroporator (Bio-Rad, Hercules, CA, USA). OD value was measured in Multiskan MK3 microplate reader (Thermo-Fisher, Waltham, MA, USA). Fluorescence intensity was measured in SpectaMax i3x micro-titer plate reader (Molecular Devices, Sunnyvale, USA). Characterization of rCDs

was performed in Nicolet IS10 FT-IR Spectrometer (Thermo-Fisher, Waltham, MA, USA), FEI Talos F200X microscope (Thermo-Fisher, Hillsboro, OR, USA), ESCALAB 250XI electron spectrometer (Thermo Scientific, Waltham, MA, USA), and FLS1000/FSS FL spectrometer (Edinburgh Instruments Ltd, Livingston, UK).

Construction of phage displayed VHH library.

Immunization was performed on a healthy alpaca in NBbiolab company (Chengdu, China). Peripheral blood mononuclear cell (PBMC) was isolated from fresh blood using lymphocyte separation medium by density gradient centrifugation. The isolated PBMC was lysed in TRNzol. The total RNA was extracted from PBMC and immediately reverse transcribed to cDNA using commercial kits. Nested PCR was performed to amplify the VHH genes. Firstly, cDNA was used as templates and CALL001 and CALL002 were used as primers to perform PCR amplification. The 750 bp DNA was obtained by gel purification and used as the templates of the second amplification with forward primer F-*SfiI*. For reverse primer, R1-*SfiI* and R2-*SfiI* were employed for IgG$_2$ and IgG$_3$ genes, respectively. All the primer sequences are shown in Table S1. The 450 bp VHH genes were gel-purified and cloned into the pComb3X vector by *SfiI* restriction sites which were introduced by primers. Recombinant vectors were transformed into fresh competent cell *E. coli* TG1 by electroporation. The transgenic cells were calculated and amplified on an agarose medium with ampicillin and then a portion of cells were cultured and infected by M13KO7 helper phage to generate phage library.

Biopanning of fenitrothion selective phage clone.

The genes of fenitrothion selective clones were selected by a simultaneous competition panning strategy [27] and the screening was performed by icELISA. All the candidate clones were sequenced to identify their amino acid sequence. Details of the protocol are shown in Supporting Information.

Preparation of biotinylated VHH.

All the positive clones were transformed into competent cell *E. coli* BL21(ED3) to express VHH through IPTG inducing. The titer, sensitivity, and cross-reactivity (CR) of positive clones were studied by icELISA to select the best performance clone. VHH genes of the selected clones were cloned into pINQ vector and transferred to *E. coli* BL21(ED3) carrying pCY216 vector with birA genes. Biotinylated VHHjd8 (VHHjd8-BT) were prepared by the protocol in Supporting Information. The organic solvent tolerance VHHjd8 and VHHjd8-BT were studied and compared with anti-fenitrothion mAb. [26]

Preparation of rCDs.

The synthesis of rCDs was referred to Qu et. al. [28] Briefly, 1 g of citric acid and 2 g of urea were dissolved in 10 mL of DMF and then the mixture was transferred to 25 mL Teflon-lined autoclave and heated to 160 °C for 6 h. The obtained dark red product was mixed with 20 mL NaOH solution (50 mg/mL), and then centrifuged 10 min at 23446×*g*. The precipitate was dissolved in water and centrifuged again to remove residual salts.

Development of FIA.

The microplate was coated with hapten 2-BSA (500 ng/mL, 100 μL/well) overnight at 37 °C and then washed twice with PBST. Afterward, 5% skimmed milk in PBS was added (120 μL/well) to block the uncoated sites for 3 h at 37 °C and the plates were dried. The series concentration of fenitrothion solutions (in PBS) was added to the microplate (50 μL/well) and the VHHjd8-BT (12.25 pg/mL in PBS (50 μL/well) was added subsequently. After 30 min incubation, the wells were washed 5 times by PBST and SA-polyHRP (100 μL/well) was subsequently added for 30 min incubation. After five times washing with PBST, TMB peroxidase substrate (100 μL/well) was added and incubated for 10 min reaction. Afterward, NaOH (pH 11, 50 μL/well) was mixed with the reaction products to adjust pH and then rCDs (50 μL/well) were subsequently added. One hundred microliter of mixture was transferred to opaque microplate and the fluorescence signal was measured with the excitation wavelength of 540 nm and emission wavelength of 610 nm.

Determination of samples.

Fenitrothion free samples (tangerines, lettuces, and Chinese cabbages) were verified by GC-MS/MS. Samples were homogenized and mixed with 10 mL of acetonitrile in a 50 mL polypropylene centrifuge tube. Four grams of $MgSO_4$, 1 g of NaCl, 1 g of sodium citrate, 0.5 g of sodium dihydrogen citrate, and a ceramic homogenizer were added and the tube was shaken vigorously for 1 min, followed by centrifuging for 5 min at $1676 \times g$. Six milliliters of the upper layer was transferred to a 15 mL polypropylene centrifuge tube with the addition of 900 mg of $MgSO_4$ and 150 mg of PSA, for 1 min vigorously shaken, followed by centrifuging for 5 min at $1676 \times g$. The extractions were filtrated by 0.22 μm membrane for GC-MS/MS analysis and 20-fold diluted for FIA analysis. The detail of GC-MS/MS was summarized in Supporting Information (Table S2).

RESULTS

Identification of alpaca antiserum.

An alpaca was immunized subcutaneously with hapten 1-LF (Figure 1A) mixed with Freund's incomplete adjuvant. After the 3rd immunization, the antiserum was characterized by icELISA. Results showed that the titer of antiserum reached the top and became stable after the 3rd immunization (Figure 1B). The conventional IgG_1 and heavy-chain-only IgG_2 and IgG_3 were separated by protein A/G using elution buffer with different pH values (Figure 1C). The obtained IgG_1 and $IgG_{2/3}$ were further characterized by icELISA. The results showed that both conventional IgG_1 and $IgG_{2/3}$ exhibited obvious titer. The inhibition rate of IgG_1 and $IgG_{2/3}$ with free fenitrothion (100 ng/mL) was 71% and 67%, respectively. This result demonstrated that the heavy chain $IgG_{2/3}$ showed satisfactory affinity to free fenitrothion (Figure 1D). The results indicated that the generation of anti-fenitrothion VHHs was successful.

Library construction of VHH library and selection of fenitrothion-specific VHHs.

The total RNA was extracted from the peripheral blood of alpaca and reversely transcribed to cDNA using commercial kits (Figure 2A and B). Then DNA of VHHs was amplified

by a Nested PCR strategy. In the first amplification, primers were designed from sequences coding the heavy chain of camelidae antibodies from heavy chain constant region 3 (CH_3) to variable regions of all kinds of IgGs. Due to the natural lack of CH_1 structural domain, the PCR products of IgG_2 and IgG_3 were only 750 bp while IgG_1 products were 1000 bp. In the second amplification, primers designed for the variable region and a portion of the hinge region of HcAbs [29] were used to amplify 750 bp DNA template to obtain VHH genes (Figure 2C).

The VHH genes were then cloned into pComb3X vectors (Figure 2D). The recombinant vectors were transformed in *E. coli* TG1 by electroporation to construct a 10^7 cfu immune library. After phage rescue, a 10^{12} cfu/mL phage library was obtained for panning. In the biopanning process, positive clones were enriched while negative clones and weak affinity clones were discarded (Figure 2E).

After careful biopanning, a total of 17 positive clones with different amino acid sequences were finally isolated (Figure S1). The 17 clones were further expressed by *E. coli* BL21(DE3) and purified. Most clones exhibited a good affinity to hapten 2-BSA and can be inhibited by free fenitrothion at low concentrations (Figure 3A). Some of them showed high CR to parathion-methyl, which can be used as a bispecific antibody for simultaneous detection of fenitrothion and parathion-methyl (Table S3).

Biotinylation of anti-fenitrothion VHH.

Based on the characterization results of the 17 VHHs, VHHjd8 exhibited the highest titer and affinity to fenitrothion and the lowest CR to analogue. The VHHjd8 gene was cloned into pINQ vector containing Avi taq, which can realize site-specific biotinylation to construct VHHjd8-BT (Figure 3B). The obtained VHHjd8-BTBT and VHHjd8 were further characterized by icELISA using SA-polyHRP. As shown in Figure S2A, an $OD_{450\,nm}$ value of 1.44 was observed for VHHjd8-BT while no titer was observed for VHHjd8 (Figure S2A). Lower working concentration (12.25 pg/mL) was used for icELISA to obtain the same working titer in comparison with the usage of anti-VHH-HRP, indicating the significant amplification of signal by SA-polyHRP. (Figure S2B).

Stability study of VHHjd8, VHHjd8-BT, and mAb.

Previous studies reported that VHHs showed high tolerance to organic solvents. [30–32] In this study, the organic solvent tolerance test of VHHjd8, VHHjd8-BT, and mAb was performed by using icELISA. In the presence of acetonitrile or acetone, the OD values observed for VHHjd8 and VHHjd8-BT were obviously higher than that of mAb (Figure 4A and C). It seems that VHHs have superior organic solvent tolerance. However, the inhibition rate of both mAb and VHHs decreased as the concentration of organic solvent increased (Figure4 B and D), which may attribute to the conformation change of biding pocket of both mAb and VHH.

Identification of rCDs.

To develop FIA, rCDs were synthesized and characterized. The rCDs showed a size of 2.7 nm and the an interplanar spacing of 0.21 nm (Figure S3A). The functional groups

on the surface of rCDs were analyzed by Fourier transform infrared spectroscopy (FT-IR) spectrum and X-ray photoelectron spectroscopy (XPS). As shown in Figure S3B, the broad bands located in 3100–3500 cm^{-1} are stretching vibration of O-H or N-H, which provided abundant hydrophilic groups to ensure the good solubility of rCDs. [28] Weak bands located at 2800~3000 cm^{-1} belong to stretching vibration of C-H. [33] The aromatic C-C (1610 cm^{-1}) and C=C (1450 cm^{-1}) demonstrate that rCDs have aromatic ring structure. [33, 34] The 1350 cm^{-1} and 1020 cm^{-1} peak indicate the C-O and C-N, respectively. [33, 35] The stretching vibration band of C-O-C located at 1000–1270 cm^{-1} demonstrated that rCDs have ether groups. [34, 36] The chemical composition was further examined by XPS. As shown in Figure S3C, the C 1s, N 1s, O 1s, and four Na element peaks (Na 1s, Na 2s, Na 2p, and Na KL1) of XPS survey spectrum were observed. The high-resolution XPS spectrum of C 1s can be decomposed into three peaks at the binding energy of 284.8 eV, 285.9 eV and 288.3 eV, corresponds to the groups of C-C/C=C, C-N/C-O/C=N, and O=C-O, respectively (Figure S3D). [34] The N 1s is decomposed into two peaks at the binding energy of 397.9 eV and 399.9 eV, corresponding to pyridine N and pyrrolic N, respectively [37] (Figure S3E). For the peak separation of O 1s, tree peaks at the binding energy of 531.5 eV, 533.5 eV, and 535.5 eV are shown in Figure S3F, which corresponds to the groups of C=O, O=C-O, and C-O on the aromatic rings, respectively. [34, 38] All the above results speculate that the rCDs might have a conjugation core in pyridine and pyrrolic form, which is the basis of long-wavelength fluorescence emission performance. [25, 34] The hydrophilic groups such as amino, hydroxyl, and carboxylic group on the surface resulted in the high solubility of rCDs.

Development of FIA based on rCDs.

The optical properties of rCDs are shown in Figure S4A, the maximum excitation and emission wavelength of rCDs are 540 nm and 610 nm, respectively. The rCDs show two absorption peaks at 330 nm and 500 nm. The oxTMB is the product from TMB-HRP system and exhibits an absorption peak at 650 nm which can overlap the emission peak of rCDs (Figure S4B). Therefore, oxTMB can quench the fluorescence of rCDs to achieve a fluorescent quenching response. Moreover, no fluorescent intensity was observed for both TMB and oxTMB, suggesting that no background interference was resulted (Figure S4C). Additionally, there is no influence to the fluorescence lifetime of rCDs after oxTMB addition, indicating that the principle of fluorescence quenching might be inner fitter effect [39] (Figure S4D).

Based on the fluorescent response mechanism, the FIA was developed by using SA-polyHRP and rCDs (Figure 5A). To be noticed, the fluorescent intensity of rCDs was affected by pH value. [34] The fluorescence intensity of rCDs in alkaline solution was significantly higher than that in the acidic solution (Figure 5B). However, the best pH value for the activity of HRP was 3.8, which would cause a decrease in fluorescent intensity of rCDs (Figure 5C). To achieve a higher response signal, serial pH solutions were added after the generation of oxTMB. As a result, the highest intensity response of rCDs to TMB was observed at the pH value of 11 (Figure 5D) and the maximum emission wavelength shift to 610 nm. Based on icELISA using SA-polyHRP, rCDs were added to oxTMB and fluorescence quenching was achieved. The fluorescent intensity showed a

good linear response with fenitrothion concentration from 0.078 ng/mL to 100 ng/mL, with correlation coefficient $R^2=0.991$ (Figure 5E). The LOD of the assay calculated by 10% increase in maximum of fluorescent intensity (IC_{10}) was 0.03 ng/mL, which was 15-fold improvement compared to conventional icELISA (Figure S5). Compared with previous studies for fenitrothion immunoassay, the developed FIA based on VHHjd8-BT was more sensitive than most of them (Table S4). In specificity study, VHHjd8-BT showed 18.5% cross-reactivity (CR) to parathion-methyl and only 1.7% CR to parathion (Table 1). For the other six analogues, CRs were less than 0.1%, suggesting the satisfactory specificity of VHHjd8-BT.

Recovery test.

The pretreatment procedure is shown in Figure S6A. After the extraction and purification steps, the extracting solutions were diluted by PBS. As shown in Figure S6B–D, the matrix effect of the three samples was removed after a 20-fold dilution. Correspondingly, a calibration curve against fenitrothion was obtained by using 5% acetonitrile. Recovery test was further studied and the results are summarized in Table 2. The recoveries of FIA and GC-MS/MS were 82.8%−114.5% and 81.8%−120%, with the coefficient of variances (CVs) of 5.7%−12.9% and 1.2%−6.3%. The results of FIA showed good agreement to GC-MS/MS, indicating good accuracy and practicability of the developed FIA.

DISCUSSION

Conventional mAb is the main element for the development of immunoassay, which however suffers from complicated cell screening, long productive period, single-function, and high cost. Owing to the excellent features of VHHs, well-designed haptens and artificial antigens [26] were employed (Figure 1A) for the generation of VHHs and the development of immunoassay. After animal immunization and serum characterization, an immune heavy-chain-only library was constructed for biopanning, which was the key step to isolate VHHs with high sensitivity and specificity. During biopanning, fenitrothion was employed as a competitor and the concentration of fenitrothion should be decreased after each round of biopanning to obtain VHHs with high sensitivity. After strict and careful biopanning, 17 VHHs were finally isolated and characterized by using icELISA. As shown in Table S3, most of these VHHs showed different specificity and affinity to fenitrothion, which was ascribed to the various complementarity-determining regions (CDRs), especially the CDR3 (Figure S1). Compared to the conserved region, it is obvious that the CDR3 of the 17 clones show various sequences and the length mainly ranges from 9–22 amino acids. Fourteen of these clones have more than 17 amino acids in CDR3 loop, which is longer than the loop in VHs from humans or mice. [40] The long CDR3 can from concave-shaped binding sites with framework region 2 (FR2) to accommodate small molecules, [41] leading to high affinity to the antigen. [42, 43] To be noticed, the sensitivity of three clones (VHHjd1, VHHjd3, and VHHjd5) were obviously lower than other clones. For VHHjd3 and VHHjd5, their CDR3 are shorter than that of other colons, which might not provide enough epitope concave to bind fenitrothion and thereby resulted in affinity decreasing. For VHHjd1, compare with other clones, it was observed that the Pro102 replaced Gly102. The Pro102 might limit the flexibility of CDR3 loop for docking and thereby resulted in the low affinity

to fenitrothion. Amount of them, VHHjd8 exhibited the lowest working concentration, indicating the highest titer. Moreover, the sensitivity and specificity of VHHjd8 were satisfactory for fenitrothion analysis. Consequently, VHHjd8 was selected for biotinylation for the following FIA development.

Previous studies have reported that VHHs show high affinity to free analytes in buffers with high concentration of organic solvent. [32, 44, 45] In this study, although VHHjd8 and VHHjd8-BT showed high titer by using organic solvents (Figure 4 A and C), no affinity improvement to fenitrothion was observed compared with mAb (Figure 4 B and D). It was assumed that the high titer observed for VHHs in organic solvents might not be attributed to the high affinity to coating antigen, but to be caused by nonspecific adsorption or other unclear mechanisms. The binding affinity of both mAb and VHHs to fenitrothion were reduced by organic solvent, which might be caused by the structure change [46] or some unknown mechanisms. In future work, the computer-assisted molecular simulation will be employed to study the corresponding mechanism and site-direct mutagenesis of VHHs will be proceeded to improve the sensitivity of VHHs in organic solvent.

Since VHHjd8-BT was not suitable for working in organic solvent, PBS was employed as working buffer for the development of FIA. To achieve high sensitivity, probes with higher signal amplification capability were required. The generated biotinylation VHHjd8-BT was employed for icELISA test by the use of SA-polyHRP instead of conventional secondary antibody-HRP and showed higher titer than that of conventional VHHs. To further improve the sensitivity of the assay, rCDs which can be quenched by oxTMB were prepared through hydrothermal. After icELISA procedure based on VHHjd8-BT-SA-polyHRP system, the prepared rCDs were subsequently added for fluorescence quenching response and finally developed a FIA method. Compared with conventional icELISA, the developed FIA showed the LOD of 0.03 ng/mL, which showed 15-fold sensitivity improvement to icELISA and obviously lower than MRLs. [6–9] Moreover, the strategy of FIA required no complicated procedure and was convenient for sensitivity improvement. The recovery test verified the accuracy and practicability of developed FIA, which was simple, sensitive, and economic for the rapid screening of fenitrothion in food samples. However, in the specificity test, VHHj8-BT showed obvious CR to parathion-methyl, which limited the specificity of VHHjd8-BT and its application. In future work, the site-directed evolution of VHHjd8 for specificity improvement will be processed based on computer-assisted molecular simulation.

Supplementary Material

Refer to Web version on PubMed Central for supplementary material.

Funding

References

[1]. Hassani S, Momtaz S, Vakhshiteh F, Maghsoudi AS, Ganjali MR, Norouzi P, et al. , Biosensors and their applications in detection of organophosphorus pesticides in the environment, Arch. Toxicol 91 (2016) 109–130, 10.1007/s00204-016-1875-8. [PubMed: 27761595]

[2]. Aragay G, Pino F, Merkoçç A, Nanomaterials for sensing and destroying pesticides, Chem. Rev 112 (2012) 5317–5338, 10.1021/cr300020c. [PubMed: 22897703]

[3]. Balali-Mood M, Balali-Mood K, Moodi M, Balali-Mood B, Health aspects of organophosphorous pesticides in asian countries, Iran. J. Public Health 41 (2012) 1–14,

[4]. Canli AG, Surucu B, Ulusoy HI, Yilmaz E, Kabir A, Locatelli M, Analytical methodology for trace determination of propoxur and fenitrothion pesticide residues by decanoic acid modified magnetic nanoparticles, Molecules 24 (2019) 4621, 10.3390/molecules24244621.

[5]. Cho YA, Seok J, Lee H, Kim YJ, Park YC, Lee YT, Synthesis of haptens of organophosphorus pesticides and development of immunoassays for fenitrothion, Anal. Chim. Acta 522 (2004) 215–222, 10.1016/j.aca.2004.05.083.

[6]. GB 2763—2021, China national food safety standard—maximum residue limits for pesticides in food,

[7]. EU Plant Pesticides database. https://ec.europa.eu/food/plant/pesticides/eu-pesticides-database/,

[8]. States Environmental Protection Agency (EPA), Code of Federal Regulations (40 CFR Part 180). https://www.govinfo.gov/content/pkg/CFR-2014-title40-vol24/xml/CFR-2014-title40-vol24-part180.xml,

[9]. Codex Alimentarius Commission Pesticide Index, http://www.fao.org/fao-who-codexalimentarius/codex-texts/dbs/pestres/pesticides/en/.

[10]. Kumar V, Vaid K, Bansal SA, Kim K, Nanomaterial-based immunosensors for ultrasensitive detection of pesticides/herbicides: Current status and perspectives, Biosens. Bioelectron 165 (2020) 112382, 10.1016/j.bios.2020.112382.

[11]. Brena BM, Arellano L, Rufo C, Last MS, Montano J, Egana CE, et al. , ELISA as an affordable methodology for monitoring groundwater contamination by pesticides in low-income countries, Environ. Sci. Technol 39 (2005) 3896–3903, 10.1021/es048620d. [PubMed: 15984762]

[12]. Xu ZL, Wang Q, Lei HT, Eremin SA, Shen YD, Wang H, et al. , A simple, rapid and high-throughput fluorescence polarization immunoassay for simultaneous detection of organophosphorus pesticides in vegetable and environmental water samples, Anal. Chim. Acta 708 (2011) 123–129, 10.1016/j.aca.2011.09.040. [PubMed: 22093354]

[13]. Ozaki CY, Silveira CR, Andrade FB, Nepomuceno R, Silva A, Munhoz DD, et al. , Single chain variable fragments produced in *Escherichia coli* against heat-labile and heat-stable toxins from enterotoxigenic *E. coli*, PLoS One 10 (2015) e131484, 10.1371/journal.pone.0131484.

[14]. Wang YA, Jiang JQ, Fotina HN, Zhang HT, Chen JJ, Advances in antibody preparation techniques for immunoassays of total aflatoxin in food, Molecules 25 (2020) 4113, 10.3390/molecules25184113.

[15]. Gonzalez-Sapienza G, Rossotti MA, Tabares-da Rosa S, Single-domain antibodies as versatile affinity reagents for analytical and diagnostic applications, Front. Immunol 8 (2017) 977, 10.3389/fimmu.2017.00977. [PubMed: 28871254]

[16]. Muyldermans S, Nanobodies: natural single-domain antibodies, Annu. Rev. Biochem 82 (2013) 775–797, 10.1146/annurev-biochem-063011-092449. [PubMed: 23495938]

[17]. Tang ZW, Wang XR, Lv JW, Hu XG, Liu X, One-step detection of ochratoxin A in cereal by dot immunoassay using a nanobody-alkaline phosphatase fusion protein, Food Control 92 (2018) 430–436, 10.1016/j.foodcont.2018.05.013.

[18]. Zarebski LM, Urrutia M, Goldbaum FA, Llama single domain antibodies as a tool for molecular mimicry, J. Mol. Biol 349 (2005) 814–824, 10.1016/j.jmb.2005.03.072. [PubMed: 15890359]

[19]. Kunz P, Flock T, Soler N, Zaiss M, Vincke C, Sterckx Y, et al. , Exploiting sequence and stability information for directing nanobody stability engineering, BBA-Gen. Subjects 1861 (2017) 2196–2205, 10.1016/j.bbagen.2017.06.014.

[20]. Schumacher D, Helma J, Schneider AFL, Leonhardt H, Hackenberger CPR, Nanobodies: chemical functionalization strategies and intracellular applications, Angew. Chem. Int. Edit 57 (2018) 2314–2333, 10.1002/anie.201708459.

[21]. Hua XD, Ding Y, Yang JC, Ma M, Shi HY, Wang MH, Direct competitive fluoroimmunoassays for detection of imidaclothiz in environmental and agricultural samples using quantum dots and europium as labels, Sci. Total Environ 583 (2017) 222–227, 10.1016/j.scitotenv.2017.01.056. [PubMed: 28117157]

[22]. Wang BL, Yu Y, Zhang HY, Xuan YZ, Chen GR, Ma WY, et al. , Carbon dots in a matrix: energy-transfer-enhanced room-temperature red phosphorescence, Angew. Chem. Int. Edit 58 (2019) 18443–18448, 10.1002/anie.201911035.

[23]. Lee C, Kwon W, Beack S, Lee D, Park Y, Kim H, et al. , Biodegradable nitrogen-doped carbon nanodots for non-invasive photoacoustic imaging and photothermal therapy, Theranostics 6 (2016) 2196–2208, 10.7150/thno.16923. [PubMed: 27924157]

[24]. Luo PG, Sahu S, Yang S, Sonkar SK, Wang J, Wang H, et al. , Carbon "quantum" dots for optical bioimaging, J. Mater. Chem. B 1 (2013) 2116–2127, 10.1039/c3tb00018d. [PubMed: 32260843]

[25]. Zhu ZJ, Zhai YL, Li ZH, Zhu PY, Mao S, Zhu CZ, et al. , Red carbon dots: Optical property regulations and applications, Mater. Today 30 (2019) 52–79, 10.1016/j.mattod.2019.05.003.

[26]. Chen ZJ, Huang ZC, Huang S, Zhao JL, Sun YM, Xu ZL, et al. , Effect of proteins on the oxidase-like activity of CeO2 nanozymes for immunoassays, Analyst 146 (2021) 864–873, 10.1039/d0an01755h. [PubMed: 33231579]

[27]. Pirez-Schirmer M, Rossotti M, Badagian N, Leizagoyen C, Brena BM, Gonzalez-Sapienza G, Comparison of three antihapten VHH selection strategies for the development of highly sensitive immunoassays for microcystins, Anal. Chem 89 (2017) 6800–6806, 10.1021/acs.analchem.7b01221. [PubMed: 28494149]

[28]. Qu SN, Zhou D, Li D, Ji WY, Jing PT, Han D, et al. , Toward efficient orange emissive carbon nanodots through conjugated sp2-domain controlling and surface charges engineering, Adv. Mater 28 (2016) 3516–3521, 10.1002/adma.201504891. [PubMed: 26919550]

[29]. Ghassabeh GH, Saerens D, Muyldermans S; Springer Berlin Heidelberg: Berlin, Heidelberg, 2010, pp 251–266.

[30]. Dona V, Urrutia M, Bayardo M, Alzogaray V, Goldbaum FA, Chirdo FG, Single domain antibodies are specially suited for quantitative determination of gliadins under denaturing conditions, J. Agric. Food Chem 58 (2010) 918–926, 10.1021/jf902973c. [PubMed: 20039674]

[31]. He T, Wang Y, Li P, Zhang Q, Lei J, Zhang Z, et al. , Nanobody-based enzyme immunoassay for aflatoxin in agro-products with high tolerance to cosolvent methanol, Anal. Chem 86 (2014) 8873–8880, 10.1021/ac502390c. [PubMed: 25079057]

[32]. Kim HJ, McCoy MR, Majkova Z, Dechant JE, Gee SJ, Tabares-da RS, et al. , Isolation of alpaca anti-hapten heavy chain single domain antibodies for development of sensitive immunoassay, Anal. Chem 84 (2012) 1165–1171, 10.1021/ac2030255. [PubMed: 22148739]

[33]. Holaá K, Sudolskaá M, Kalytchuk S, Nachtigallová D, Rogach AL, Otyepka M, et al. , Graphitic nitrogen triggers red fluorescence in carbon dots, ACS Nano 11 (2017) 12402–12410, 10.1021/acsnano.7b06399. [PubMed: 29136460]

[34]. Zhang XQ, Chen CY, Peng DP, Zhou YZ, Zhuang JL, Zhang XJ, et al. , pH-Responsive carbon dots with red emission for real-time and visual detection of amines, J. Mater. Chem. C 8 (2020) 11563–11571, 10.1039/d0tc02597f.

[35]. Gu L, Zhang JR, Yang GX, Tang YY, Zhang X, Huang XY, et al. , Green preparation of carbon quantum dots with wolfberry as on-off-on nanosensors for the detection of Fe^{3+} and l-ascorbic acid, Food Chem. 376 (2022) 131898, 10.1016/j.foodchem.2021.131898.

[36]. Tan CL, Zhou C, Peng XY, Zhi HZ, Wang D, Zhan QQ, et al. , Sulfuric Acid Assisted Preparation of Red-Emitting Carbonized Polymer Dots and the Application of Bio-Imaging, Nanoscale Res. Lett 13 (2018) 10.1186/s11671-018-2657-4.

[37]. Wu ZL, Xiong ZK, Liu R, He CS, Liu Y, Pan ZC, et al. , Pivotal roles of N-doped carbon shell and hollow structure in nanoreactor with spatial confined Co species in peroxymonosulfate activation: Obstructing metal leaching and enhancing catalytic stability, J. Hazard. Mater 427 (2022) 128204, 10.1016/j.jhazmat.2021.128204.

[38]. Chen YQ, Sun XB, Wang XY, Pan W, Yu GF, Wang JP, Carbon dots with red emission for bioimaging of fungal cells and detecting Hg^{2+} and ziram in aqueous solution, Spectrochim. Acta A 233 (2020) 118230, 10.1016/j.saa.2020.118230.

[39]. Dong BL, Li HF, Mujtaba Mari G, Yu XZ, Yu WB, Wen K, et al. , Fluorescence immunoassay based on the inner-filter effect of carbon dots for highly sensitive amantadine detection in foodstuffs, Food Chem. 294 (2019) 347–354, 10.1016/j.foodchem.2019.05.082. [PubMed: 31126473]

[40]. Tu Z, Huang X, Fu J, Hu N, Zheng W, Li Y, et al. , Landscape of variable domain of heavy-chain-only antibody repertoire from alpaca, Immunology 161 (2020) 53–65, 10.1111/imm.13224. [PubMed: 32506493]

[41]. He T, Nie Y, Yan TT, Zhu J, He XL, Li Y, et al. , Enhancing the detection sensitivity of nanobody against aflatoxin B_1 through structure-guided modification, Int. J. Biol. Macromol 194 (2022) 188–197, 10.1016/j.ijbiomac.2021.11.182. [PubMed: 34863829]

[42]. Li C, Tang ZO, Hu ZX, Wang YW, Yang XM, Mo FZ, et al. , Natural single-domain antibody-nanobody: a novel concept in the antibody field, J. Biomed. Nanotechnol 14 (2018) 1–19, 10.1166/jbn.2018.2463. [PubMed: 29463363]

[43]. Qiu L, Feng Y, Ma X, Li J, A camel anti-lysozyme CDR3 only domain antibody selected from phage display VHH library acts as potent lysozyme inhibitor, Acta Bioch. Bioph. Sin 49 (2017) 513–519, 10.1093/abbs/gmx037.

[44]. Fu HJ, Wang Y, Xiao ZL, Wang H, Li ZF, Shen YD, et al. , A rapid and simple fluorescence enzyme-linked immunosorbent assay for tetrabromobisphenol A in soil samples based on a bifunctional fusion protein, Ecotox. Environ. Safe 188 (2020) 109904, 10.1016/j.ecoenv.2019.109904.

[45]. He T, Wang YR, Li PW, Zhang Q, Lei JW, Zhang ZW, et al. , Nanobody-based enzyme immunoassay for aflatoxin in agro-products with high tolerance to cosolvent methanol, Anal. Chem 86 (2014) 8873–8880, 10.1021/ac502390c. [PubMed: 25079057]

[46]. Horá ek J, Skládal P, Effect of organic solvents on immunoassays of environmental pollutants studied using a piezoelectric biosensor, Anal. Chim. Acta 412 (2000) 37–45, 10.1016/S0003-2670(00)00756-X.
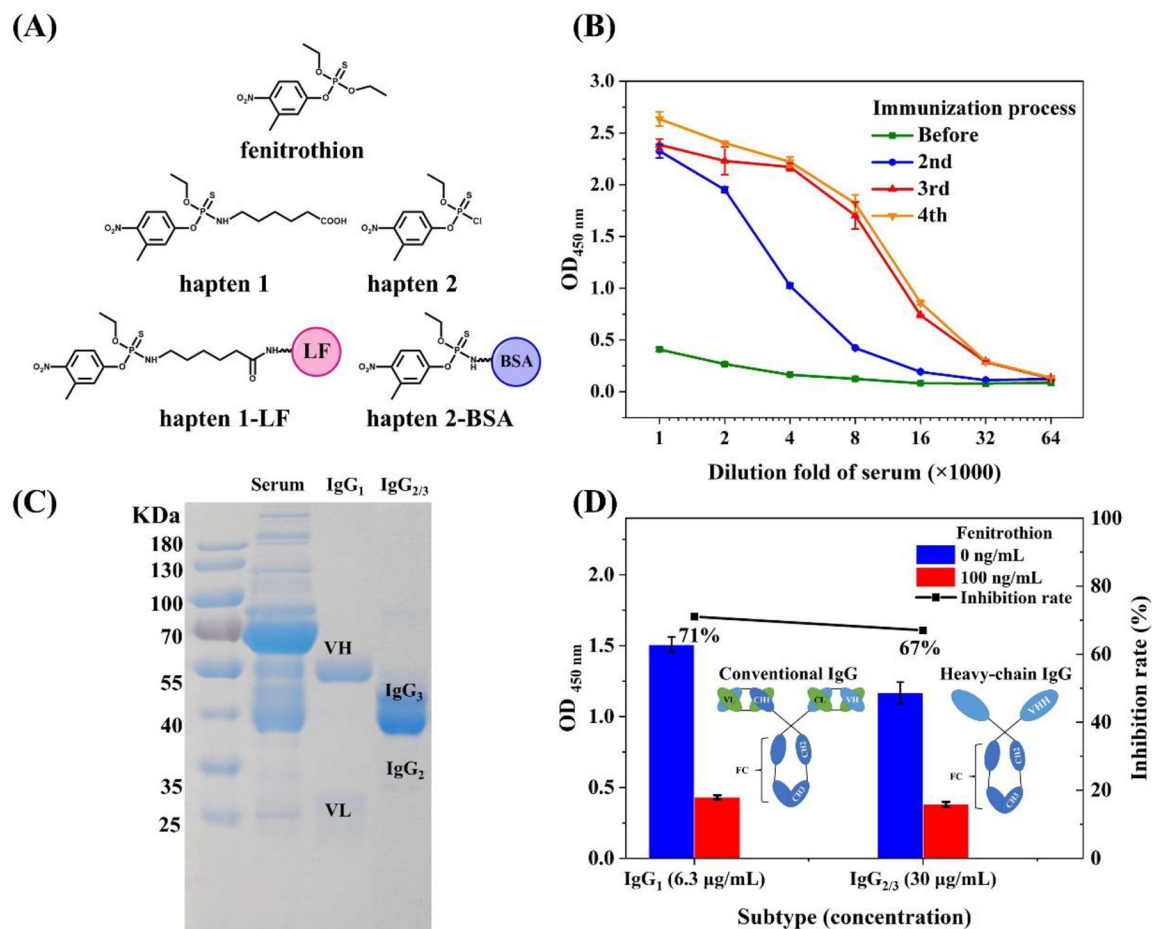
Figure 1.
(A) Structure of haptens and artificial antigens for fenitrothion; (B) Characterization of alpaca serum by indirect ELISA; (C) SDS-PAGE IgGs subtypes isolated from alpaca serum; (D) Characterization of conventional IgG and heavy-chain IgG by icELISA. The inhibition rate for fenitrothion of IgG_1 and $IgG_{2/3}$ was 71% and 67%, respectively.
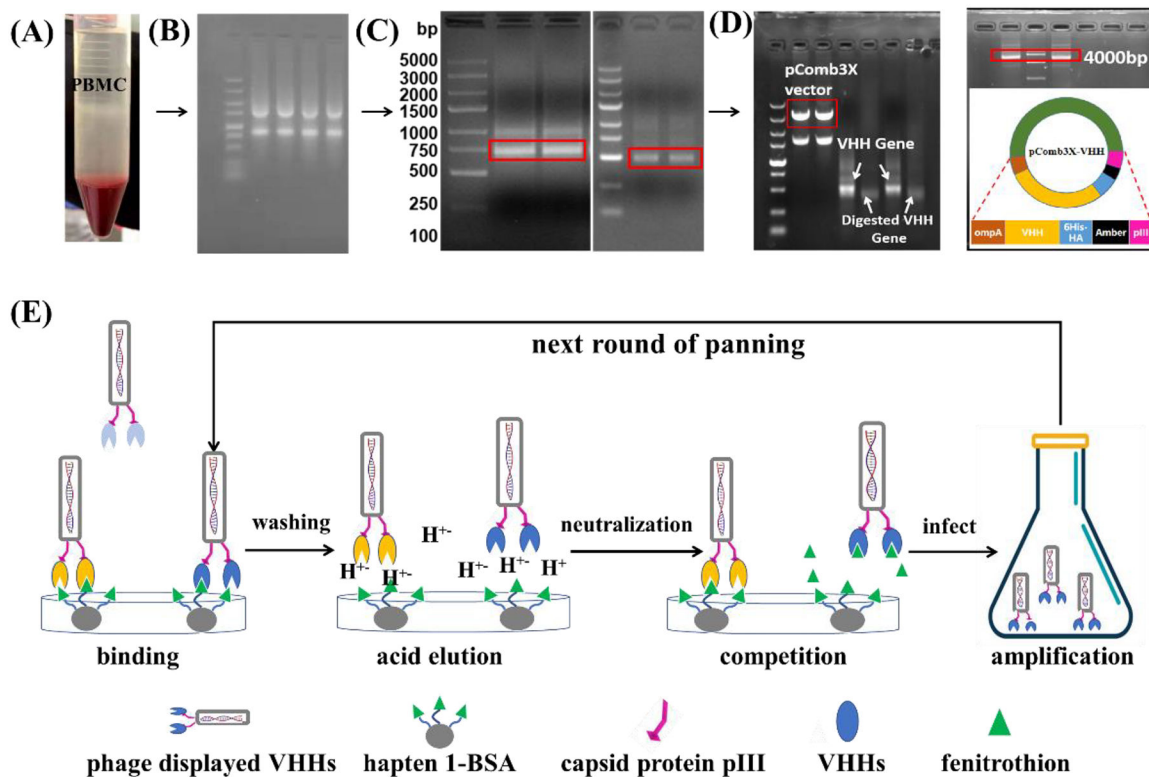
Figure 2.
Construction of VHHs gene library and bio-panning procedure. (A) Isolation of PBMC isolation; (B) Extraction of RNA; (C) Amplification of VHH genes; (D) Construction of expression vectors; (E) Bio-panning and phage display.
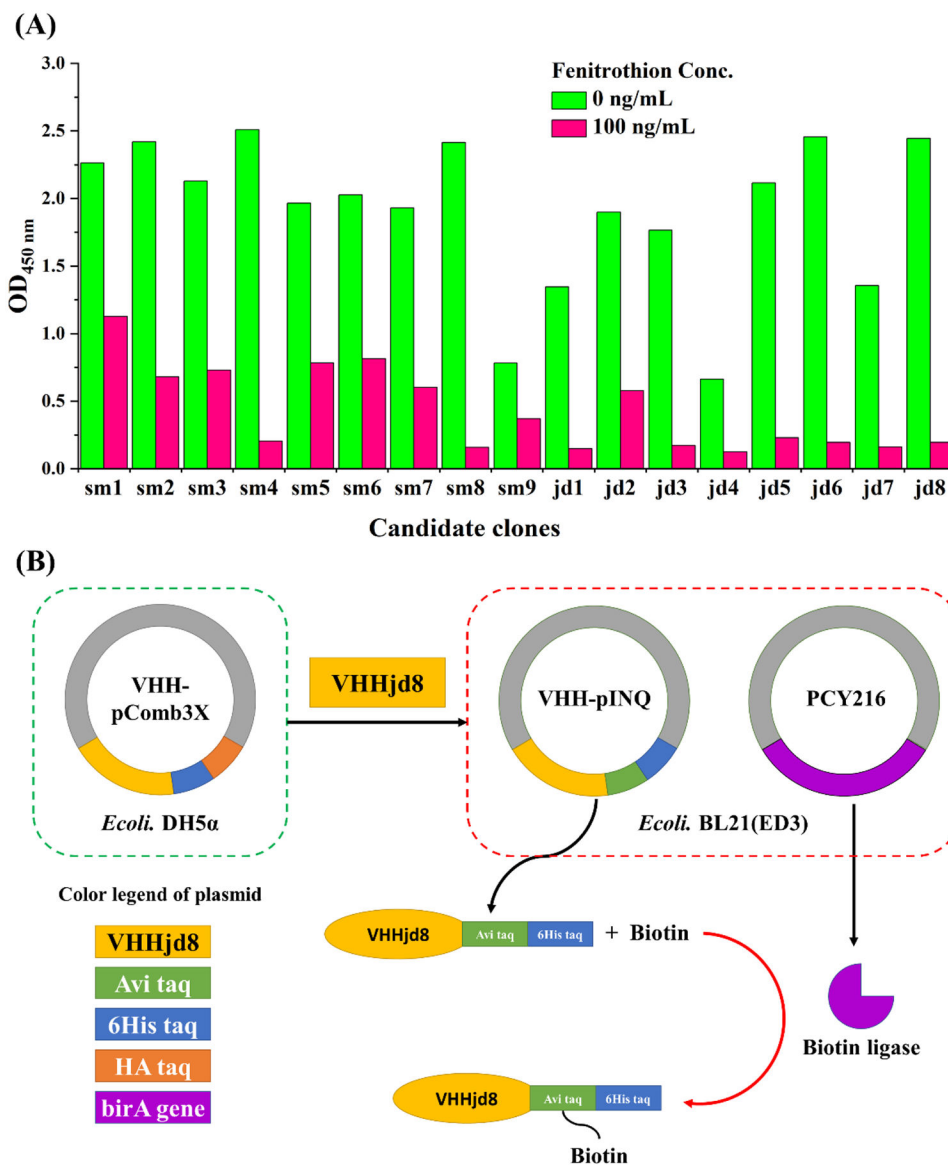
Figure 3.
(A) Candidate clones identified by indirect competitive ELISA with (100 ng/mL) and without (0 ng/mL) the presence of fenitrothion; (B) The principle of production of VHHjd8-BT.
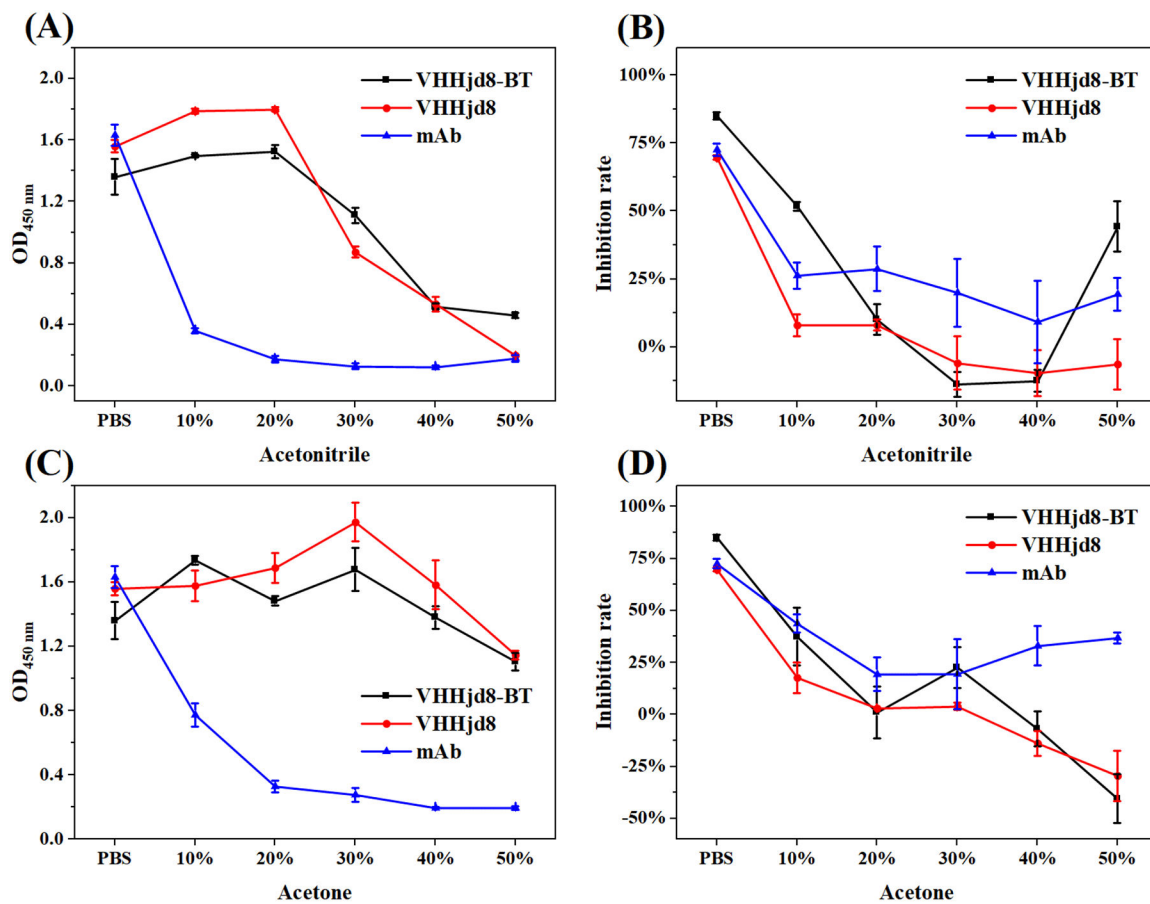
Figure 4.
Stability study of anti-fenitrothion VHHjd8 and the corresponding mAb. Effect of acetonitrile on binding activity to (A) hapten 2-BSA and (B) inhibition rate; Effect of acetone on binding activity to (C) hapten 2-BSA and (D) inhibition rate.
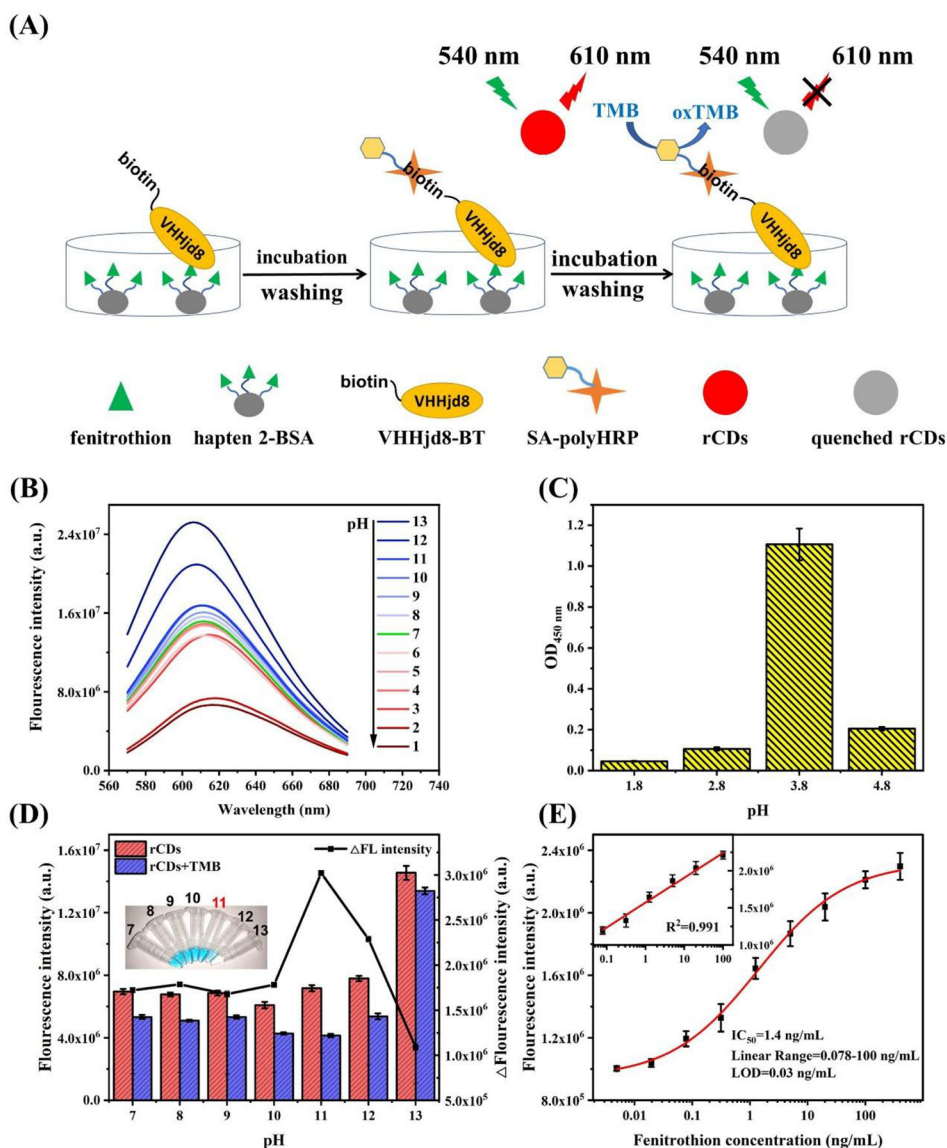
Figure 5.
(A) Protocol of fluorescence immunoassay based on rCDs quenching; (B) Fluorescence intensity of rCDs combined with NaOH/HCl with different pH; (C) Effects of pH on HRP activity; (D) rCDs quenched by oxTMB with different pH; (E) Calibration curve of the FIA assay (n=3).

Table 1

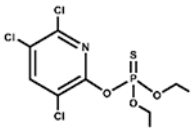Cross-reactivity (CR) for fenitrothion and its analogue by VHH-based FIA
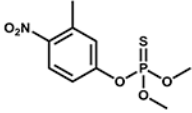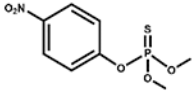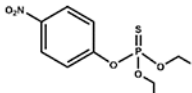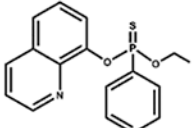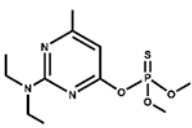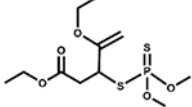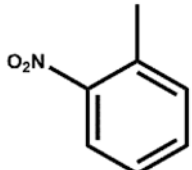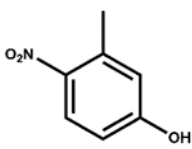
Analyte	Structure	IC$_{50}$ (ng/mL)	CR (%)
Fenitrothion		1.4	100
Parathion-methyl		7.4	18.5
Parathion		82.4	1.7
Chloroyrifos		>10000	<0.1
Quintiofos		>10000	<0.1
Pirimiphos-methyl		>10000	<0.1
Malathion		>10000	<0.1
2-Nitrotoluene		>10000	<0.1
3-Methyl-4-nitrophenol		>10000	<0.1

Table 2

Recovery of fenitrothion from spiked food samples by proposed FIA (n=3)

Sample	Spiked (ng/g)	FIA			GC-MS/MS		
		Measured Mean ± SD[a] (ng/g)	Recovery (%)	CV[b] (%)	Measured Mean ± SD (ng/g)	Recovery (%)	CV (%)
Chinese cabbage	2.0	1.8±0.1	88.8	10.0	2.4±0.04	120.0	1.7
	20.0	22.0±2.8	110.2	12.9	20.2±0.8	101.0	4.0
	200.0	180.3±15.0	90.2	8.3	163.5±2.4	81.8	1.5
Lettuce	2.0	1.7±0.2	86.7	12.2	2.4±0.04	120.0	1.7
	20.0	16.6±1.7	82.8	10.3	22.5±0.8	112.5	3.6
	200.0	184.3±12.5	92.2	6.8	189.9±2.5	95.0	1.3
Tangerine	2.0	1.9±0.2	97.3	11.8	2±0.08	100.0	4.0
	20.0	22.9±1.3	114.5	5.7	19.1±1.2	95.5	6.3
	200.0	166.7±15.6	83.3	9.3	184.6±2.3	92.3	1.2

[a] SD, standard deviation.

[b] CV, coefficient of variance, which was obtained from intra-assay.